

Zero-Shot Neural Architecture Search: Challenges, Solutions, and Opportunities

Guihong Li, *Student Member, IEEE*, Duc Hoang, *Student Member, IEEE*,
Kartikya Bhardwaj, *Member, IEEE*, Ming Lin, *Member, IEEE*,
Zhangyang Wang, *Senior Member, IEEE*, Radu Marculescu, *Fellow, IEEE*

Abstract—Recently, *zero-shot* (or *training-free*) Neural Architecture Search (NAS) approaches have been proposed to liberate the NAS from training requirements. The key idea behind zero-shot NAS approaches is to design proxies that predict the accuracies of the given networks without training network parameters. The proxies proposed so far are usually inspired by recent progress in theoretical deep learning and have shown great potential on several NAS benchmark datasets. This paper aims to comprehensively review and compare the state-of-the-art (SOTA) zero-shot NAS approaches, with an emphasis on their hardware awareness. To this end, we first review the mainstream zero-shot proxies and discuss their theoretical underpinnings. We then compare these zero-shot proxies through large-scale experiments and demonstrate their effectiveness in both hardware-aware and hardware-oblivious NAS scenarios. Finally, we point out several promising ideas to design better proxies. Our source code and the related paper list are available on <https://github.com/SLDGroup/survey-zero-shot-nas>.

Index Terms—Neural Architecture Search, Zero-shot proxy, Hardware-aware neural network design

1 INTRODUCTION

In recent years, deep neural networks have made significant breakthroughs in many applications, such as recommendation systems, image classification, and natural language modeling [1], [2], [3], [4], [5], [6], [7]. To automatically design high performance deep networks, *Neural Architecture Search* (NAS) has been proposed during the past decade [8], [9], [10], [11], [12]. Specifically, NAS boils down to solving an optimization problem with specific targets (*e.g.*, high classification accuracy) over a set of possible candidate architectures (search space) within a group of computational budgets. Recent breakthroughs in NAS simplify the trial-and-error manual architecture design process and discover new deep network architectures with better performance and efficiency over hand-crafted ones [10], [11], [13], [14], [15], [16], [17], [18], [19], [20], [21], [22], [23], [24], [25], [26], [27], [28]. Therefore, NAS has attracted significant attentions from both academia and industry.

One important application of NAS is to design hardware efficient deep models under various constraints, such as memory footprint, inference latency and power consumption [29]. Roughly, existing NAS approaches can be categorized into three groups as shown in Fig. 1: multi-shot NAS, one-shot NAS and zero-shot NAS. Multi-shot NAS methods involve training multiple candidate networks and are therefore time-consuming. It can take from a few hundred GPU hours [30] to thousands of GPU hours [31] in multi-shot NAS methods. One-shot NAS methods alleviate the

computational burden by sharing candidate operations via a hyper-network [11], [32], [33], [34], [35], [36], [37]. As shown in Fig. 2, one-shot NAS only needs to train a single hyper-network instead of multiple candidate architectures whose number is usually exponentially large. The orders of magnitude reduction in training time enables differentiable search to achieve competitive accuracy against multi-shot NAS, but with much lower search costs [11].

Nevertheless, naively merging all candidate operations into a hyper-network is not efficient because the parameters of all operations need to be stored and updated during the search process. Consequently, the *weight-sharing* methods improve the search efficiency of NAS even further [13], [39], [40], [41], [42]. As shown in Fig. 3, the key idea of weight-sharing NAS is to share the parameters across different operations. Next, at each training step, a sub-network is sampled from the hyper-network and then the updated parameters are copied back to the hyper-network. By sharing the parameters of various sub-networks, this differentiable search approach significantly reduces the search costs to a few or tens of GPU hours [39].

Though the differentiable search and weight-sharing have significantly improved the time efficiency of NAS, training is still required in one-shot NAS methods. In the last few years, the *zero-shot* NAS has been proposed to liberate NAS from parameter training entirely [43], [44], [45], [46], [47], [48], [49], [50], [51], [52].

Compared to multi-shot and one-shot methods, zero-shot NAS has the following major advantages: (i) **Time efficiency**: zero-shot NAS utilizes some proxy as the model’s test accuracy to eliminate the model training altogether during the search stage. Compared to model training, the computation costs of these proxies are much more lightweight. Therefore, zero-shot NAS can significantly reduce the costs of NAS while achieving comparable test accuracy as one-shot and

- Guihong Li, Duc Hoang, Zhangyang Wang, and Radu Marculescu are with the Department of Electrical and Computer Engineering, The University of Texas at Austin, TX, 78712. E-mail: {lgh, hoangduc, atlaswang, radum}@utexas.edu
- Kartikya Bhardwaj is with Qualcomm AI Research, an initiative of Qualcomm Technologies, Inc., CA, 92121. E-mail: kbhardwa@qti.qualcomm.com
- Ming Lin is with Amazon, WA, 98004. E-mail: minglamz@amazon.com.
- Correspondence to Radu Marculescu (radum@utexas.edu).

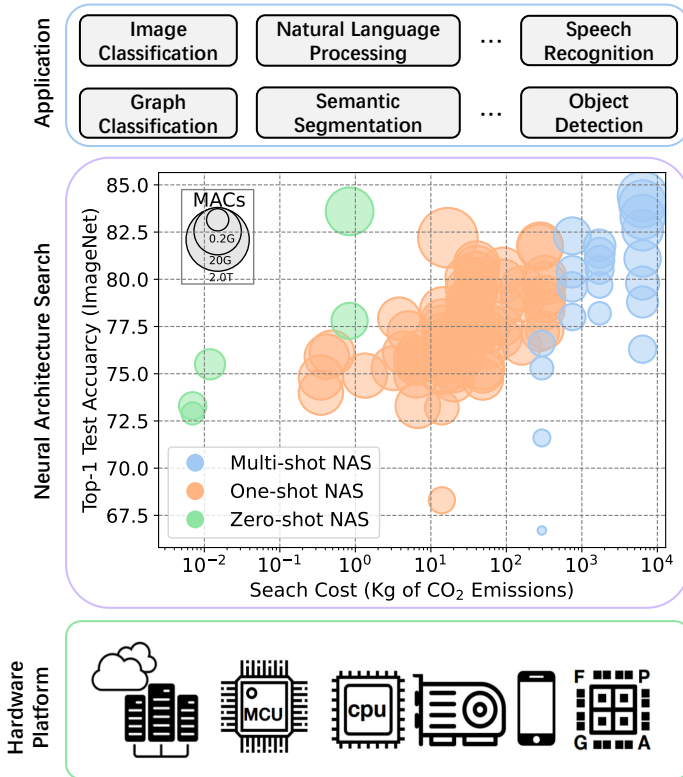


Fig. 1: Overview of existing NAS approaches. NAS is designed to search for optimal architectures with both good accuracy and high efficiency on real hardware. (Data collected from [38])

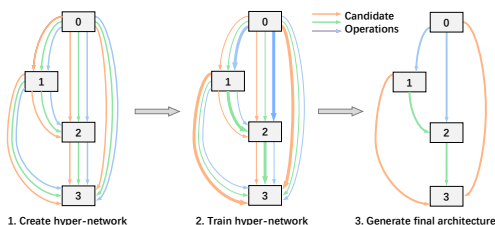


Fig. 2: Illustration of differentiable neural architecture search. (1). Merge all candidate operations into a hyper-network with learnable weights for each operation. (2). Train the hyper-network and update the learnable weights for each operation. (3) Generate the final results by selecting the operations with the highest weight values (boldest edges). (Adapted from [11])

multi-shot NAS approaches (see Fig. 1). (ii) **Explainability:** Clearly, the quality of the accuracy proxy ultimately determines the performance of zero-shot NAS. The design of an accuracy proxy for zero-shot NAS is usually inspired by some theoretical analysis of deep neural networks thus deepening the theoretical understanding of why certain networks may work better. For instance, some recent approaches use the number of linear regions to approximate the complexity of a deep neural network [53]. Moreover, the connection between the gradient of a network at random initialization and the accuracy of that network after training are widely explored in zero-shot NAS [54].

Based on these overarching observations, this paper aims

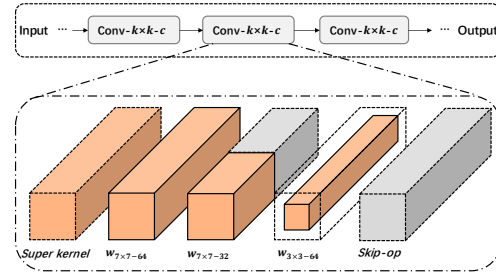


Fig. 3: Illustration of weight-sharing mechanism. The parameters of relatively simple operations are obtained from complex operations, *i.e.*, super kernel. As shown, different operations share the parameters from the super kernel. (Adapted from [39])

to comprehensively analyze existing hardware-aware zero-shot NAS methods. Starting from the theoretical foundations of deep learning, we first investigate various proxies of test accuracy and their theoretical underpinnings. Then, we introduce several popular benchmarks for evaluating zero-shot NAS methods. Moreover, we demonstrate their effectiveness when applied to hardware-aware NAS; notably, we reveal fundamental limitations of existing proxies. Finally, we discuss several potential research directions for hardware-aware zero-shot NAS. Overall, this paper makes the following contributions:

- We review existing proxies for zero-shot NAS and provide theoretical insights behind these proxies. We categorize the existing accuracy proxies into (i) gradient-based proxies and (ii) gradient-free proxies.
- We conduct direct comparisons of various zero-shot proxies against two naive proxies, *i.e.*, #Params and #FLOPs, and reveal a fundamental limitation of many existing proxies: they correlate much worse with the test accuracy in constrained search settings (*i.e.*, when considering only networks of high accuracies) compared to unconstrained settings (*i.e.*, considering all architectures in the given search space).
- We further conduct a thorough study including proxy design, benchmarks, and real hardware profiling for zero-shot NAS. We show that a few proxies have a better correlation with the test accuracy than these two naive proxies (#Params and #FLOPs) on the top-performing architectures such as ResNets and MobileNets.
- We discuss the limitations of existing zero-shot proxies and NAS benchmarks; we then outline a few possible directions for future research.

Of note, compared to other existing zero-shot NAS surveys [55], [56], [57], [58], [59], [60], [61], [62], we not only cover all existing proxies, but also provide a deep analysis of the theoretical underpinning behind them. We believe that understanding the theoretical design considerations behind these proxies is very important for future improvements. Moreover, for the first time, we conduct detailed comparisons when applying zero-shot NAS to hardware-aware scenarios. This is crucial for deploying the zero-shot approaches in practice, especially for edge-AI applications.

The remainder of this paper is organized as follows. We introduce zero-shot proxies in Section 2. Section 3 surveys existing NAS benchmarks. Hardware latency predictor is presented in Section 3.3. We evaluate various zero-shot proxies under hardware-aware settings in Section 4 and point out future research directions. We conclude the paper in Section 5.

2 ZERO-SHOT PROXIES

The goal of zero-shot NAS is to design proxies that can rank the accuracy of candidate network architectures at the initialization stage, *i.e.*, without training, such that we can replace the expensive training process in NAS with some computation-efficient alternatives. Hence, the proxy for the accuracy ranking is the key factor of zero-shot NAS.

In [61], the existing accuracy proxies are classified into two classes: (i) data-dependent, where the accuracy proxy is calculated over the real data of the target task; (ii) data-independent, where the proxy’s value doesn’t rely on the real data. In this paper, we categorize zero-shot proxies from another perspective: depending on whether or not the gradients are involved in proxy’s calculation, the existing accuracy proxies fall into two major classes: (i) gradient-based accuracy proxy and (ii) gradient-free accuracy proxy (summarized in Table 1). The symbols used in this section and their corresponding meaning are summarized in Table 2.

2.1 Gradient-based accuracy proxies

We first introduce several similar proxies derived from the gradient over parameters of deep networks.

2.1.1 Gradient norm

The gradient norm is the sum of norms for each layer’s gradient vector [54]. To calculate the gradient norm, we first input a mini-batch of data into the network and then propagate the loss values backward. Next, we calculate the ℓ_2 -norm of each layer’s gradient and then add them up for all the convolution and linear layers of the given network. Formally, the definition of gradient norm G is as follows:

$$G \triangleq \sum_{i=1}^D \|\nabla_{\theta_i} L\|_2 \quad (1)$$

where D , θ_i and L are, the number of layers, the parameter vector of the i -th layer of a given network and L is the loss values, respectively.

2.1.2 SNIP

The gradient norm only measures the property of the gradient’s propagation for a given network. To jointly measure the parameter importance both in forward inference and gradient propagation, SNIP consists of multiplying the value of each parameter and its corresponding gradient [63]. Formally, SNIP is defined as below:

$$\text{SNIP} \triangleq \sum_i^D |\langle \theta_i, \nabla_{\theta_i} L \rangle| \quad (2)$$

where $\langle \rangle$ represents for inner product; D , θ_i and L are, the number of layers, the parameter vector of the i -th layer of a given network and L is the loss values, respectively.

2.1.3 Synflow

Similar to SNIP, Synflow consists of maintaining the sign of the SNIP proxy [64]:

$$\text{Synflow} \triangleq \sum_i^D \langle \theta_i, \nabla_{\theta_i} L \rangle \quad (3)$$

2.1.4 GraSP

The above three proxies only take the first-order derivatives of neural networks into account. The GraSP proxy considers both the first-order and second-order derivatives of neural networks [65]. Specifically, GraSP multiplies the gradient and Hessian matrix of parameters:

$$\sum_i^D -\langle \mathbf{H}_i \nabla_{\theta_i} L, \theta_i \rangle \quad (4)$$

where \mathbf{H}_i is Hessian matrix of the i -th layer.

There are multiple theoretical analyses for the above three proxies. Specifically, Synflow and SNIP have been proven to be layer-wise constants in linear networks during the back-propagation process [63], [64]. Moreover, authors in [65], [66] show that Synflow and GraSP are different approximate formats of the first-order Taylor expansion of deep neural networks. We remark that the Taylor expansion of a deep network can identify the parameters that contribute the most to the loss values; thus, it can measure the importance of parameters.

Besides the gradient over parameters, the gradient over each layer’s activation is also explored to build the accuracy proxy as shown below.

2.1.5 Fisher information

Authors of [67] show that Fisher information of a neural network can be approximated by the square of the activation value and their gradients:

$$\sum_i^D \langle \nabla_{z_i} L, z_i \rangle^2 \quad (5)$$

where z_i is the feature map vector of the i -th layer of a given network.

Previous works show that a second-order approximation of Taylor expansion in a neural network is equivalent to an empirical estimate of the Fisher information [67]. Hence, measuring the Fisher information of each neuron/channel of a given network can reflect the importance of these neurons/channels.

2.1.6 Jacobian covariant

Besides the gradient over parameters and activations, the Jacobian covariant (Jacob_cov) leverages the gradient over the input data \mathbf{x} [68], [69]. To get the Jacob_cov proxy, given an input batch with B input samples $\{\mathbf{x}_1, \mathbf{x}_2, \dots, \mathbf{x}_B\}$, the gradients matrix \mathbf{J} of the output results $\{y_1, y_2, \dots, y_B\}$ vs. these inputs is first computed:

$$\mathbf{J} = (\nabla_{\mathbf{x}_1} y_1, \nabla_{\mathbf{x}_2} y_2, \dots, \nabla_{\mathbf{x}_B} y_B)^T \quad (6)$$

Next, the raw covariance matrix is generated as:

$$\mathbf{G} = (\mathbf{J} - \mathbf{M})(\mathbf{J} - \mathbf{M})^T \quad (7)$$

TABLE 1: Categorization of zero-shot accuracy proxies. Based on whether the proxy relies on gradients or not, there are gradient-based and gradient-free approaches. According to whether the computations of proxy rely on the real data from the dataset or not, there are data-dependent or data-independent approaches.

	Gradient-based	Gradient-free
Data-dependent	Grad_norm, SNIP, Synflow, GraSP, Fisher, Jacob_cov, NTK_Cond	-
Data-independent	Zen-score	#LR, NN-Mass

TABLE 2: The symbols used in this paper and their corresponding meaning.

Symbol	Meaning	Symbol	Meaning
\mathbf{x}	Input samples	\mathbf{y}^T	Ground truth (labels)
f	A given deep network	D	The number of layers of a given network
f_e	A network w/o final pooling and FC layers	\mathbf{y}	The output of a given model
L	loss values	$\boldsymbol{\theta}_i$	Parameters vector of the i -th layer
\mathbf{H}_i	Hessian matrix of the i -th layer	\mathbf{z}_i	The output vector of layer i

where $M_{i,j} = \frac{1}{B} \sum_{n=1}^B J_{i,n}$. Then the raw covariance matrix is normalized to get the real covariance matrix Γ :

$$\Gamma_{i,j} = \frac{G_{i,j}}{\sqrt{G_{i,i}G_{j,j}}} \quad (8)$$

where $\Gamma_{i,j}$ denotes the entries of Γ . Let $\lambda_1 \leq \lambda_2 \leq \dots \leq \lambda_B$ be the B eigenvalues of Γ ; then the Jacobian covariant is generated as follows:

$$\text{Jacob_cov} \triangleq - \sum_{i=1}^B \left[(\lambda_i + \epsilon) + (\lambda_i + \epsilon)^{-1} \right] \quad (9)$$

where ϵ is a small value used for numerical stability. As discussed in [68], [69], Jacob_cov can reflect the expressivity of deep networks thus higher Jacob_cov values indicate better accuracy.

2.1.7 Zen-score

Zen-score is a new proxy for a given model [70], [71]. The Zen-score is defined as:

$$\log \mathbb{E}_{\mathbf{x}, \epsilon} (\|f_e(\mathbf{n}) - f_e(\mathbf{n} + \alpha\epsilon)\|_F) + \sum_{k,i} \log \left(\sqrt{\frac{\sum_j \sigma_{ij}^k}{Ch_i}} \right), \quad (10)$$

$$\mathbf{x} \sim \mathcal{N}(0, \mathbf{I})$$

where, \mathbf{n} is a sampled Gaussian random vector, ϵ is a small input perturbation, $\|\cdot\|_F$ indicates the Frobenius norm, α is a tunable hyper-parameter, Ch_i is the number of channels of the i -th convolution layer, and σ_{ij}^k is the variance of the i -th layer's j -th channels for the k -th samples in an input batch data. As shown in Eq.10, Zen-score measures model expressivity by averaging the Gaussian complexity under randomly sampled x and ϵ . We note that this is equivalent to computing the expected gradient norm of f with respect to input x instead of network parameters. Hence, Zen-score measures the expressivity of neural networks instead of their trainability: networks with a higher Zen-score have a better expressivity and thus tend to have a better accuracy.

2.1.8 NTK Condition Number

Neural Tangent Kernel is proposed to study the training dynamics of neural networks [72]. More precisely, given two input samples \mathbf{x}_1 and \mathbf{x}_2 , NTK is defined as:

$$\kappa(\mathbf{x}_1, \mathbf{x}_2) = \mathbf{J}(\mathbf{x}_1)\mathbf{J}(\mathbf{x}_2) \quad (11)$$

where $\mathbf{J}(\mathbf{x})$ is the Jacobian matrix evaluated at the sample \mathbf{x} [73]. Authors in [74] prove that the training dynamics of wide neural networks can be solved as follows:

$$\mu_t(\mathbf{x}_{train}) = \left(\mathbb{I} - e^{-\eta\kappa(\mathbf{x}_{train}, \mathbf{x}_{train})t} \right) \mathbf{y}_{train} \quad (12)$$

where t denotes the training step; μ_t represents the output expectations at training step t ; \mathbf{x}_{train} and \mathbf{y}_{train} are the training samples and their corresponding labels; η is the learning rate. By conducting the eigendecomposition of Eq. 12, the i -th dimension in the eigenspace of output expectation can be written as follows:

$$\mu_t(\mathbf{x}_{train,i}) = \left(\mathbf{I} - e^{-\eta\lambda_i t} \right) \mathbf{y}_{train,i}, i = \{1, 2, \dots, m\} \quad (13)$$

where $\lambda_1 \leq \lambda_2 \leq \dots \leq \lambda_m$ are the eigenvalues of the NTK $\mathcal{K}(\mathbf{x}_{train}, \mathbf{x}_{train})$. Therefore, a smaller difference between λ_1 and λ_m indicates (on average) a more "balanced" convergence among different dimensions in the eigenspace. To quantify the above observation, the NTK Condition Number (NTK_Cond) is defined as follows [53]:

$$\text{NTK_Cond} \triangleq \mathbb{E}_{\mathbf{x}_{train}, \Theta} \frac{\lambda_m}{\lambda_1} \quad (14)$$

where Θ is the randomly initialized network parameters. Authors of [53] demonstrate that the NTK_Cond is negatively correlated with the architecture's test accuracy. Hence, the networks with lower NTK_Cond values tend to have a higher test accuracy. Similar insights are reported and leveraged in [75] for NAS of vision transformers (ViTs).

2.2 Gradient-free accuracy proxy

Though the gradient-based proxies do not require the training process on the entire dataset, backward propagation is still necessary to compute the gradient. To entirely remove the gradient computation from the neural architecture search, several gradient-free proxies have been proposed lately.

2.2.1 Number of linear regions

The number of linear regions of a network quantifies how many regions a given network could divide the input space into; thus, it describes the expressivity of a given network [76], [77], [78]. For instance, a single-neuron perceptron with a ReLU activation function can divide its input space into two regions. [79] proves that one can estimate

the number of linear regions with the help of the activation patterns of the output activation matrix R :

$$R = \mathbf{1} \cdot \mathbf{1}^T - \text{sign}[z_i(1 - z_i)^T + (1 - z_i)z_i^T] \quad (15)$$

where $\mathbf{1}$ is a all-one vector. Next, by removing the repeating patterns and assigning the weights to each pattern, the number of linear regions ρ is as follows:

$$\rho \triangleq \sum_j \frac{1}{\sum_k R_{j,k}} \quad (16)$$

where $R_{j,k}$ is the entry of R . Therefore, the number of linear regions measures how many unique regions the network can divide the entire activation space into (see Fig. 4).

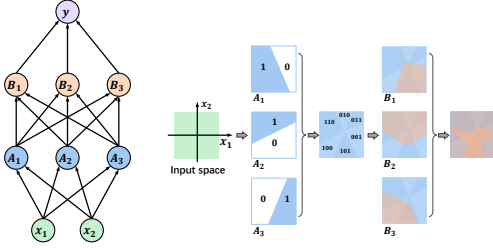


Fig. 4: The illustration of Logdet proxy; $A_i, B_i, i = \{1, 2, 3\}$ are the neurons of a multi-layer perceptron. First, the input space is divided into several linear regions. Next, each region is encoded by a binary code; then Eq. 17 is applied to compute the Logdet proxy. (Adapted from [69])

2.2.2 Logdet

Logdet is another proxy proposed based on the number of linear regions [69]:

$$H = \begin{bmatrix} N_{LR} - d_H(c_1, c_1) & \dots & N_{LR} - d_H(c_1, c_N) \\ \dots & \dots & \dots \\ N_{LR} - d_H(c_N, c_1) & \dots & N_{LR} - d_H(c_N, c_N) \end{bmatrix} \quad (17)$$

Logdet $\triangleq \log |H|$

where N_{LR} is the total number of linear regions, d_H is the Hamming distance, and c_i is the binary coding vector of the i -th linear region as shown in Fig. 4. Previous work shows that networks with a higher Logdet at initialization tend to have higher test accuracy after training [69].

2.2.3 Topology inspired proxies

The very first pioneering work behind theoretically-grounded, training-free architecture design was done by Bhardwaj et al. [80]. While the above proxies are proposed for a general search space, *i.e.*, without any constraints on the candidate architectures, as discussed later, these general-purpose proxies are not better than some naive proxies, *e.g.*, the number of parameters (#Params) of a model. To design better accuracy proxies than #Params, Bhardwaj et al. [80] constrained the search space to specific topologies, *e.g.*, DenseNets, ResNets, MobileNets, etc., and theoretically studied how network topology influences gradient propagation. Inspired by the network science, NN-Mass is defined as follows [80]:

$$\rho_c \triangleq \frac{\# \text{Actual skip connections of cell } c}{\# \text{Total possible skip connections of cell } c} \quad (18)$$

$$\text{NN-Mass} \triangleq \sum_{\text{each cell } c} \rho_c w_c d_c$$

where w_c and d_c are the width and depth values of a cell¹, respectively. Authors of [80] prove that higher NN-Mass values indicate better trainability of networks and faster convergence rate during training. Moreover, they also show that networks with higher NN-Mass values tend to achieve a higher accuracy. NN-Mass has also been used to perform training-free model scaling to significantly improve accuracy-MACs tradeoffs compared to highly accurate models like ConvNets [81]. In [81], the authors show the connection between NN-Mass and expressive power of deep networks for ResNet-type networks.

As an extension of NN-Mass, NN-Degree is proposed by relaxing the constraints on the width of networks. Formally, NN-Degree is defined as follows [82]:

$$\text{NN-Degree} = \sum_{\text{each cell } c} \left(w_c + \frac{\# \text{Actual skip connections}}{\# \text{Total input channels}} \right) \quad (19)$$

where w_c is the average width value of a cell c . Similarly to NN-Mass, NN-Degree has shown a high positive correlation with the test accuracy.

Lately, [83] developed another principled understanding of a neural network’s connectivity patterns on its capacity or trainability. Specifically, the authors theoretically characterized the impact of connectivity patterns on the convergence of deep networks under gradient descent training with fine granularity, by assuming a wide network and analyzing its Neural Network Gaussian Process (NNGP) [84]. The authors prove that how the spectrum of an NNGP kernel propagates through a particular connectivity pattern would affect the bounds of the convergence rates. On the practical side, they show that such NNGP-based characterization could act as a simple filtration of “unpromising” connectivity patterns, to significantly accelerate the large-scale neural architecture search without any overhead.

3 BENCHMARKS AND PROFILING MODELS

NAS benchmarks have been proposed to provide a standard test kit for fair evaluation and comparisons of various NAS approaches [85], [86], [87], [88]. A NAS benchmark defines a set of candidate architectures and their test accuracy or hardware costs. We classify the existing NAS benchmarks as standard NAS (*i.e.*, without hardware costs) and hardware-aware NAS benchmarks. Next, we introduce these two types of NAS benchmarks.

3.1 Standard NAS Benchmarks

3.1.1 NASBench-101

NASBench-101 provide users with 423k neural architectures and their test accuracy on the CIFAR10 dataset; the architectures are built by stacking a cell for multiple times [89]. The cells in the NASBench-101 search space can have at most seven operations; each operation is sampled from the following three operations: 3×3 convolution, 1×1 convolution, and max pooling.

¹ A cell represents a group of layers with the same width values or commonly used blocks in CNN, *e.g.*, Basic/Bottleneck blocks in ResNet, and Inverted bottleneck blocks in MobileNet-v2.

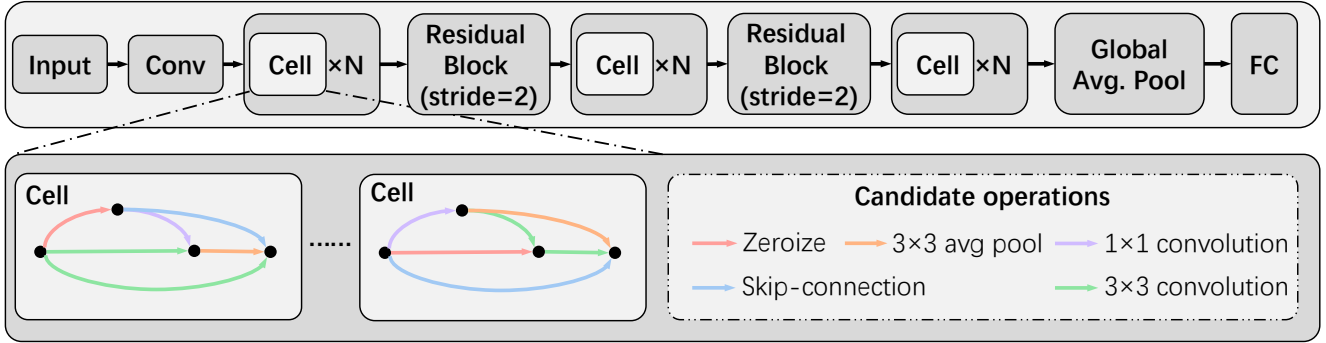


Fig. 5: Search space of NASBench-201. Each architecture in the search space is built by stacking a cell multiple times; each cell can have six operations (edges in the figure) and each operation has 5 potential different options (drawn with different colors). (Adapted from [11])

3.1.2 NATS-Bench

NATS-Bench have two different search space. *NATS-Bench-TSS* is also called NASBench-201. Similar to the NASBench-101, the networks in NASBench-201 are also built by repeating a cell multiple times [90]. One of the advantages of NASBench-201 over NASBench-101 is that NASBench-201 provides test accuracy on more datasets, namely, CIFAR10, CIFAR100, and ImageNet16-120. As shown in Fig. 5, the cells in the NASBench-101 search space have six operations; each operation is sampled from the following five operations: null, skip connection, 3×3 convolution, 1×1 convolution, and 3×3 average pooling. Therefore, there are $5^6 = 15625$ network architectures in the NASBench-201 benchmark.

NATS-Bench-SSS is the succeeding version of NASBench-201: it contains 32768 architectures with different width values for each layer; in the rest of the paper, we use the NATS-Bench to represents NATS-Bench-SSS for short [91].

3.1.3 TransNAS-Bench-101

TransNAS-Bench-101 is a benchmark dataset containing network performance on seven diverse vision tasks, including image classification, image reconstruction, and pixel-level prediction [92]. As for the candidate architectures, there are two different sub-search spaces: (i) A cell-level search space consisting of 4,096 unique networks with different cells; each cell has six operations which is sampled from the following four operations: null, skip connection, 1×1 convolution, and 3×3 convolution. (ii) A macro-level search space containing 3256 unique networks with different depths (number of blocks, varying from 4 to 6), locations of down-sample layers and widening layers.

3.2 Hardware-aware NAS benchmarks

The above benchmarks do *not* consider hardware constraints. Recent hardware-aware NAS approaches aim to jointly optimize the test performance and hardware efficiency of neural architectures. Hence, hardware-aware NAS benchmarks have been proposed by incorporating the hardware costs of networks into the search process.

HW-NAS-Bench covers the search space from both the NASBench-201 and FBNet [93]. It provides all the architectures in these two search spaces measured/estimated hardware cost (*i.e.*, latency and energy consumption) on six

different types of devices: NVIDIA Jetson TX2 (EdgeGPU), RaspberryPi-4, Google Edge-TPU, Pixel-3 phone, ASIC-Eyeriss, and Xilinx ZC706 (FPGA)).

3.3 Hardware Performance Models

To involve the hardware-awareness into NAS, we also need to construct models to efficiently and accurately estimate the hardware performance (*e.g.*, latency) of given networks. In this section, we consider latency to characterize the hardware performance and use NASBench-201 as an example to compare several representative approaches for hardware performance models.

TABLE 3: Comparison of representative hardware performance models. The granularity refers to the level of input features for the hardware performance models. Transferability refers to how efficiently the model of one hardware platform can be transferred to another new hardware. The latency is measured on Snapdragon-888’s GPU with NASBENCH-201 on CIFAR100 dataset.

Approach	Method	Granularity	Transferability	RMSE (ms)
BRP-NAS [94]	GCN/MLP	Layer	Low	4.6
HELP [95]	GCN/MLP	Layer	High	0.12
NN-Meter [96]	GCN	Kernel	Low	1.2

BRP-NAS is a pioneering approach that uses deep learning to build hardware performance models [94]. Specifically, BRP-NAS first converts a neural network into a directed acyclic graph by modeling each layer as an edge in a graph and modeling the input/output as nodes in the graph. Next, by using different values to present different types of layers, BRP-NAS uses a Graph-convolution-network (GCN) to build the hardware performance models. Then the model is trained with multiple networks and their real hardware performance data on the target hardware. In particular, for the networks with fixed depth, BRP-NAS can also use MLP to build the performance model. Though BRP-NAS can achieve good prediction results with enough training samples, there is a limitation for BRP-NAS: the performance model is trained for a specific hardware platform; if new hardware comes, one needs to repeat the entire process.

To address the above problem, HELP builds the hardware performance models by taking the hardware information as extra input features (*e.g.*, type of the hardware, number of

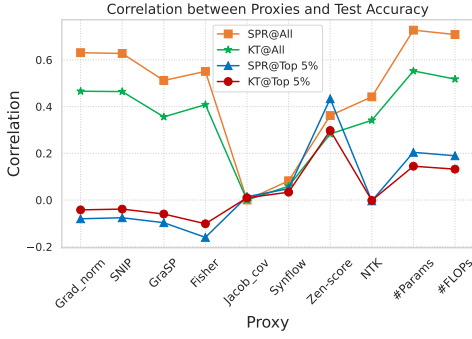


Fig. 6: The correlation between various proxies vs. test accuracy on NASBench-201 search space for CIFAR-100 dataset (averaged over 5 seeds). All: all the networks in the benchmark; Top 5%: the architectures with test accuracy ranking top 5% in the entire search space. KT and SPR are short for Kendall’s τ and Spearman’s ρ , respectively (same for Fig. (7,8,9)).

computing elements, and the size of on-chip memory) [95]. Next, HELP is trained with the latency data collected from multiple platforms, such as desktop CPU/GPU and mobile CPU/GPU. This way, if new hardware comes in, HELP only needs a few samples to conduct the fine-tuning process (typically around 10). Hence, HELP is very efficient in terms of the transferability for new hardware. Nevertheless, both BRP-NAS and HELP are built on the layer-level analysis, which is relatively coarse for an accurate prediction.

To further improve the accuracy of performance models, NN-Meter is proposed by analyzing the neural network at a finer granularity during run-time. Specifically, NN-Meter computes the kernels of each neural network, which are originally generated during the compilation process [96]. To remove the necessity of the compilation process, NN-Meter utilizes the algorithm to automatically predict the generated kernels. Hence, as shown in Table 3, NN-Meter has a much higher prediction quality than both HELP and BRP-NAS.

4 EXPERIMENTAL RESULTS

In this section, we compare the existing proxies on multiple NAS benchmarks under various scenarios. Besides the proxies mentioned above, we also evaluate two naive proxies, *i.e.*, #Params and #FLOPs.

4.1 NAS without hardware-awareness

To compare the performance of these proposed accuracy proxies, we calculate the correlation of these proxy values vs. the real test accuracy. We next discuss the results on two NAS benchmarks: NASBench-201 and NATS-Bench.

4.1.1 Unconstrained search space

We first investigate the performance of zero-shot proxies for the unconstrained search spaces, *i.e.*, considering all networks in the benchmarks.

NASBench-201: We calculate the correlation coefficients between multiple proxies and the test accuracy on CIFAR-100 and ImageNet16-120 datasets. As shown in Fig. 6 and 7,

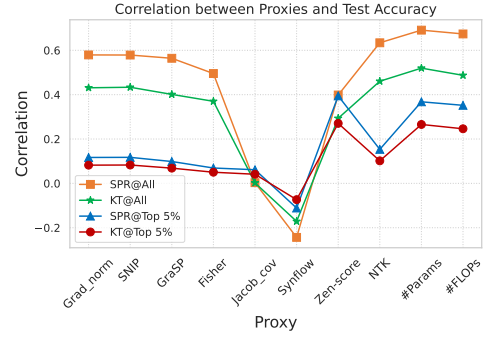


Fig. 7: The correlation between various proxies vs. test accuracy on NASBench-201 search space for ImageNet16-120 dataset (averaged over 5 seeds).

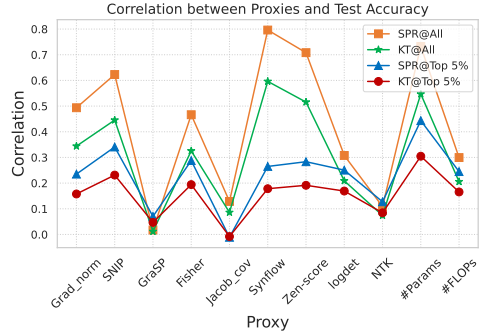


Fig. 8: The correlation between various proxies vs. test accuracy on NATS-Bench search space for CIFAR100 dataset (averaged over 5 seeds).

the #Params generally works best for these two datasets. Except for the #Params, several gradient-based proxies, such as Grad_norm, SNIP, GraSP, and Fisher, also work well.

As shown in Table 4, we compare the neural architectures with the highest test accuracy found via various proxies. The neural architectures obtained via #Params and #FLOPs have the highest test accuracy on NASBench-201, which is a natural and expected result given the correlation results above.

NATS-Bench: Similar to NASBench-201, we calculate the

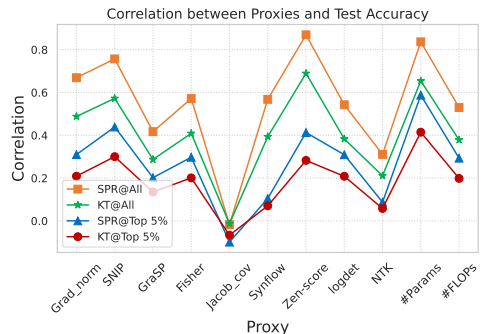


Fig. 9: The correlation between various proxies vs. test accuracy on NATS-Bench search space for ImageNet16-120 dataset (averaged over 5 seeds).

TABLE 4: The test accuracy (%) of optimal architectures obtained by various zero-shot proxies (average on 5 runs) on NASBench-201 (NB201) and NATS-Bench (NB201) for CIFAR100 (C100) and ImageNet16-120 (Img16) datasets. The best results are shown with bold fonts.

Proxies		Ground Truth	Grad_norm	SNIP	GraSP	Fisher	Jacob_cov	Synflow	Zen-score	#Params	#FLOPs
NB201	C100	73.51	60.02	60.02	60.02	60.02	68.89	62.22	68.10	71.11	71.11
	Img16	47.31	29.27	29.27	5.46	29.27	25.07	26.08	40.77	41.44	41.44
NATS	C100	70.92	48.44	68.36	57.40	53.14	55.04	66.84	69.92	70.28	70.280
	Img16	46.73	40.97	45.63	33.97	35.80	35.03	35.37	46.27	44.73	44.73

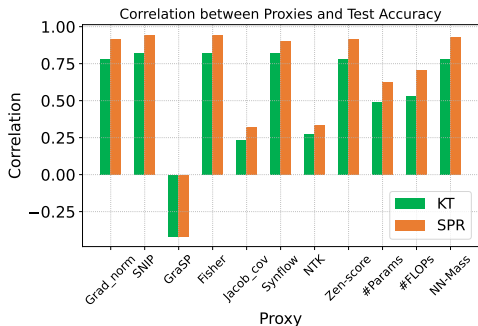


Fig. 10: The correlation between various proxies vs. test accuracy on a set of ResNets and Wide-ResNets for ImageNet dataset (averaged over 5 seeds).

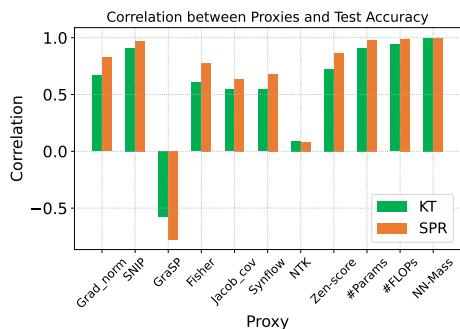


Fig. 11: The correlation between various proxies vs. test accuracy on a set of MobileNet-v2-based networks for ImageNet dataset (averaged over 5 seeds).

correlation coefficients between these proxies and the test accuracy on CIFAR-100 and ImageNet16-120 datasets for NATS-Bench. As shown in Fig. 8 and 9, the #Params and Zen-score generally work best for these two datasets.

Overall, it appears that all these proposed accuracy proxies do not have a higher correlation with the test accuracy compared to #Params and #FLOPs for these two NAS benchmarks.

4.1.2 Constrained search space

We note that the architectures with high accuracy are much more important than those networks with low test accuracy. Hence, we calculate the correlation coefficient for the architectures with test accuracy ranking top 5% in the entire search space. Fig. 6 and 7 show that, compared to ranking without constraints (*i.e.*, considering all architectures), the correlation score has a significant drop except for the Zen-score on NASBench-201. Similarly, on NATS-Bench, Fig. 8 and 9 show

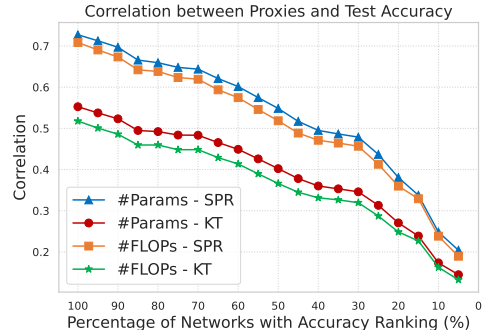


Fig. 12: The correlation between #Params & #FLOPs vs. test accuracy under various ratios of networks on NASBench-201 for CIFAR100 dataset (averaged over 5 seeds). 20% means computing the correlation scores only for the networks whose test accuracy ranks top 20% in the benchmark; 100% means considering all the networks in the benchmark (same for Fig. 13). From left to right, the search space is more and more constrained to neural architectures with high accuracy.

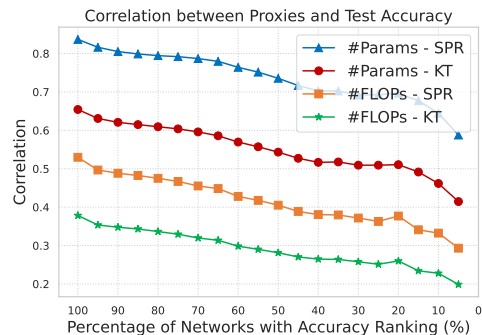


Fig. 13: The correlation between #Params & #FLOPs vs. test accuracy under various ratios of networks on NATS-Bench for ImageNet16-120 dataset (averaged over 5 seeds).

that most of the proxies have a significant correlation score drop when constrained to the top 5% networks in the search space, including #Params and #FLOPs. This correlation score drop on the top 5% networks will make the zero-shot NAS likely to miss the optimal or near-optimal networks. Table 4 shows that there is a big accuracy gap between the ground truth and the networks obtained by each proxy. These results get even worse for a search with more relaxed hardware constraints (see Sec 4.2).

As shown in previous literature, #Params and #FLOPs outperform other proxies in multiple benchmarks [62]. Hence, we dig deep into the effectiveness of #Params and #FLOPs

by gradually making the search space more constrained. As shown in Fig. 12 and Fig. 13, if we compute the correlation for networks with higher accuracy, both #Params, and #FLOPs have a significant drop in correlation score.

Given the above results, we conclude that all of the existing proxies (including #Params and #FLOPs) do *not* correlate well for the network with high accuracy. This is a fundamental drawback because what matters most for NAS are precisely these networks with high accuracy. Hence, there is great potential for designing better proxies that could yield high correlation scores for these top networks.

4.1.3 Specific Network Families

We remark that most NAS benchmarks only contain cell-based architectures, where many popular architectures are not included. Hence, in this section, we consider several commonly used networks family as the search space since they are widely used in various applications. As shown in Fig. 10, if we search within networks from ResNet and Wide-ResNet family, then SNIP, Zen-score, #Params, #FLOPs, and NN-Mass have a significantly high correlation with the test accuracy (*i.e.*, Spearman’s $\rho > 0.9$).

As shown in Fig. 11, Grad_norm, SNIP, Fisher, Synflow, Zen-score and NN-Mass work best for the MobileNet-v2 network family, which is slightly better than the two naive proxies #Params and #FLOPs. These results show that there is great potential in designing good proxies for a constrained yet widely-used search space.

In practice, the test accuracy is not the only design consideration. Indeed, the models obtained by NAS shall meet some hardware constraints, especially for deployment on edge devices. Hence, we next explore the performance of these proxies for the hardware-aware search scenarios.

4.2 Hardware-aware NAS

In this part, we conduct the hardware-aware NAS using the zero-shot proxies introduced above. Specifically, we use these zero-shot proxies other than the real test accuracy to search for the Pareto-optimal networks under various constraints. We next introduce the results on NASBench-201 (with HW-NAS-Bench) and NATS-Bench.

4.2.1 NASBench-201 / HW-NAS-Bench

We use EdgeGPU (NVIDIA Jetson TX2) as the target hardware and use the energy consumption data from HW-NAS-Bench; then we set various energy consumption values as the hardware constraints. Next, we use different accuracy proxies to traverse all candidate architectures in the search space and obtain the Pareto-optimal networks under various energy constraints.

To illustrate the quality of these networks, we plot these networks and the ground truth results obtained via actual accuracy in Fig. 14. As shown, when the energy constraint is tight (*e.g.*, less than 10mJ), most of the proxies could find networks very close to the real Pareto-optimal except the Jacob_cov. However, when the energy constraint is more relaxed (*e.g.*, more than 20mJ), only #Params, #FLOPs, and Jacob_cov can find several networks close to the ground truth.

4.2.2 NATS-Bench

We measure the latency data on NVIDIA GTX-1080 for NATS-Bench. We then use different accuracy proxies to traverse all candidate architectures to obtain the Pareto-optimal networks under various latency constraints. As shown in Fig. 15, we plot these networks and the ground truth results. When we set the latency constraint to around 50ms, only #Params, SNIP, and Zen-score can still find the networks that nearly match the real Pareto-optimal networks.

The results on these two benchmarks further verify that current proxies don’t correlate well for networks with high accuracy because the real Pareto-optimal networks have higher accuracy when the hardware constraints are more relaxed. This observation suggests a great potential to design better proxies in this scenario.

4.3 Discussion and future work

4.3.1 NAS Benchmarks

Diversity of search space: We remark that the search space of most existing NAS benchmarks only contains cell-based neural architectures. To further improve the generality of NAS benchmarks, the community may need to incorporate new architectures from more diverse search spaces. For instance, the NATS-Bench has added architectures with different cells for different stages of the search space. Moreover, the cells in these existing benchmarks are similar to the DARTS cell structure. However, in practice, the inverted bottleneck blocks from MobileNet-v2 are more widely used for higher hardware efficiency. Therefore, the next direction of NAS benchmarks may need to cover a more practical and widely used search space, such as FBNet-v3.

Awareness of hardware efficiency: So far, only HW-NAS-Bench provides multiple hardware constraints on several types of hardware platforms, but it does not have the accuracy data for most of the networks in the benchmark. Therefore, we suggest that future NAS benchmarks provide both accuracy and hardware metrics on typical hardware platforms.

4.3.2 Zero-shot proxies

Why #Params works: As shown in Section 4.1.1, #Params achieves a higher correlation than other proxies with multiple datasets and multiple benchmarks for unconstrained search space. One may wonder why such a trivial proxy works so well. In general, a good neural architecture should satisfy the following properties: good convergence/trainability and high expressive capacity. We provide the following observations:

- **Trainability** On the one hand, given similar depth, the wider networks have better trainability and higher convergence rates, and clearly more parameters [97]. On the other hand, most of the networks evaluated on popular benchmarks share a similar depth value. Hence, within these benchmarks, more parameters will also indicate a better trainability.
- **Expressivity** It’s well known that the models with more parameters are generally able to approximate more complex functions [98]. Hence, more parameters capture the higher expressive capacity of a given network.

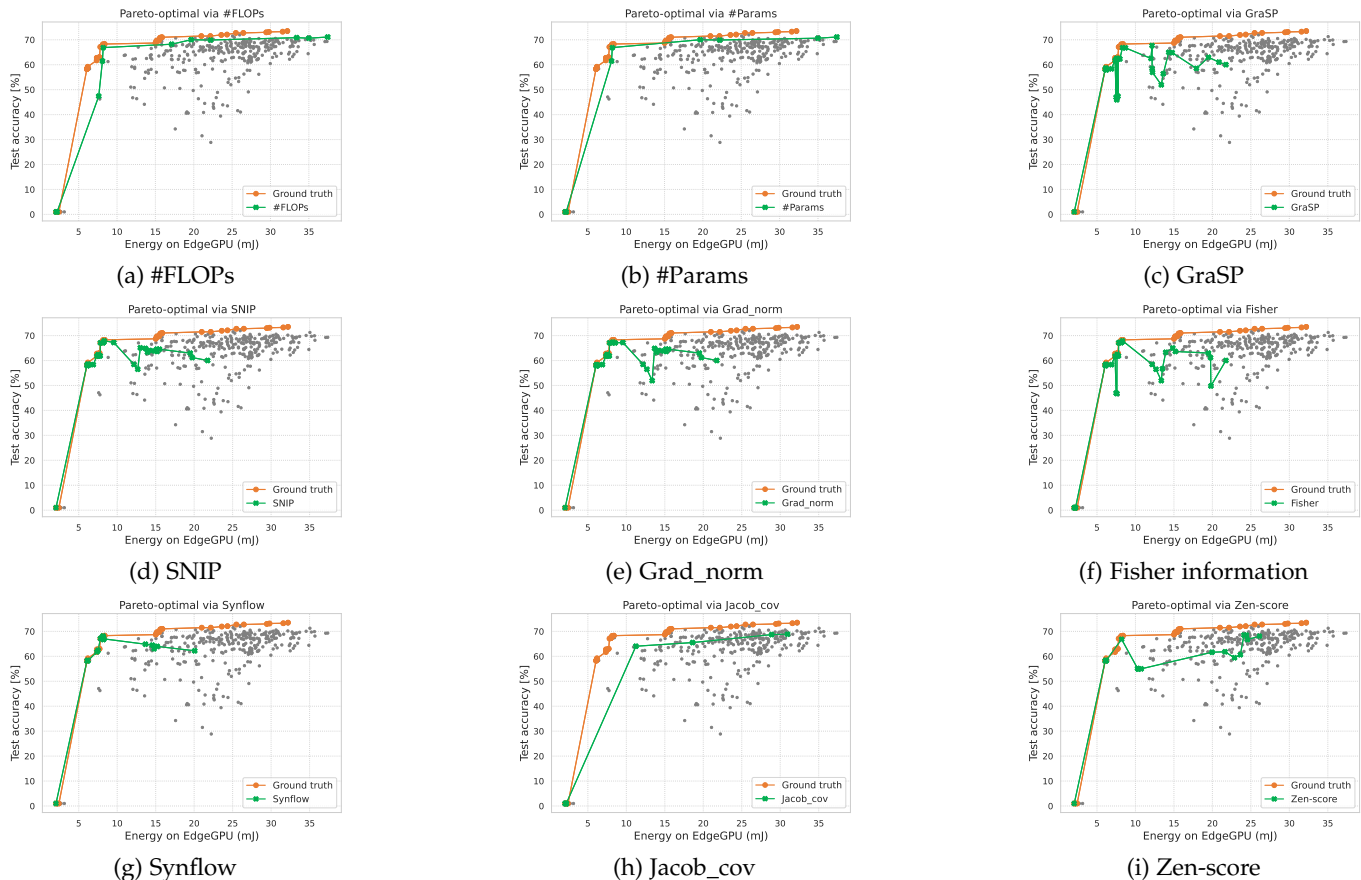


Fig. 14: Pareto-optimal networks obtained via various proxies for CIFAR100 dataset on NASBench-201, and for various energy consumption constraints on an EdgeGPU (NVIDIA Jetson TX2). The gray points in these figures are candidate networks in the search space.

Hence, #Params captures both the expressivity and trainability of the networks in these benchmarks. In contrast, most of the proposed proxies usually emphasize either the expressivity or the trainability of networks (but not both). That may be why #Params outperforms these proposed proxies. Hence, future work should try to design a proxy that could indicate both the convergence/trainability and expressive capacity of a given network. For instance, recently propose proxy ZiCo indicates both trainability and generalization capacity of neural networks thus consistently outperforming #Params in multiple NAS benchmarks.

When #Params fails: (i) As shown in this section when accounting for the architectures with test accuracy ranking top 5%, several proxies outperform both #Params and #FLOPs for some benchmarks. Furthermore, these top-performing network architectures are most important since NAS focuses on obtaining the networks with high accuracy. (ii) Many proxies work well on the constrained search space, such as MobileNet and ResNet families. These networks are widely used in many applications (e.g., MobileNet-v2 for EdgeAI). Clearly, the above two failing cases are very important to push zero-shot NAS to more practical scenarios. Hence, there is a great potential to explore better zero-shot proxies in the above cases.

Search method: Though #Params outperforms most proxies in several scenarios in terms of correlation coefficients, there are

alternative search methods to use these zero-shot proxies. For example, as demonstrated in [53], to better leverage these proxies, one potential search method can merge all candidate networks into a supernet and then apply these proxies to prune the network at the initialization stage until hardware constraints are met. This way, the time efficiency of zero-shot NAS approaches can be further improved since the search space is gradually compressed with pruning going on.

Theoretical support: We remark that most gradient-based proxies are first proposed to estimate the importance of each parameter or neuron/channel of a given network, thus originally applied to the model pruning problem space instead of ranking networks. Hence, the effectiveness of these gradient-based proxies for zero-shot NAS needs a more profound understanding from a theoretical perspective. Moreover, though most gradient-free proxies are usually presented with some theoretical analysis for NAS, as shown in Section 4.1 and Section 4.2, they generally have a lower correlation with the gradient-based ones. The theoretical understanding of why these zero-shot proxies can or cannot estimate the test accuracy of different networks is still an open question.

Customized proxy for different types of networks: As mentioned in Section 4.1.3, several zero-shot proxies do not work well for a general search space, but do show a great correlation with the test accuracy and beat the #Params on constrained

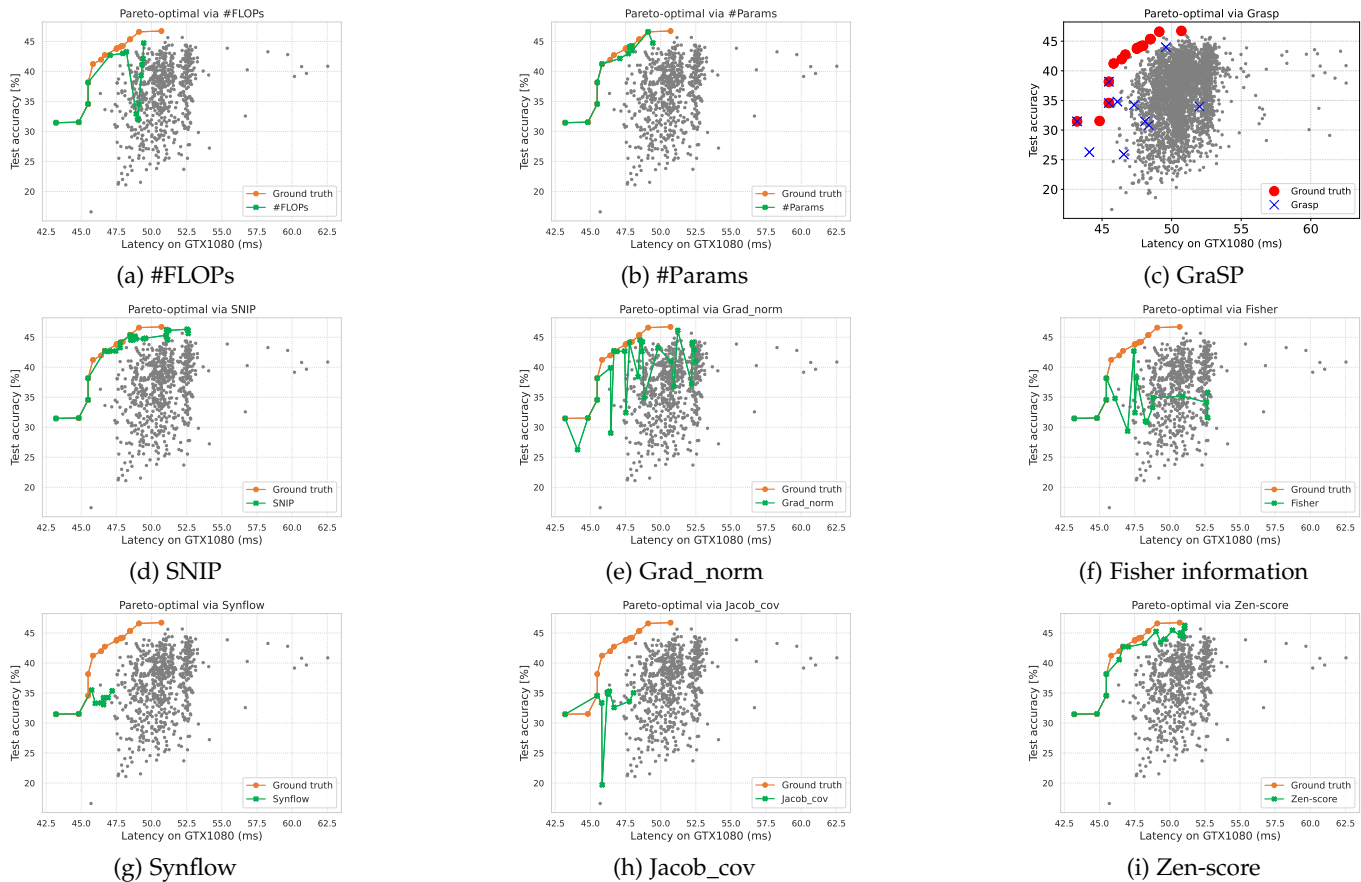


Fig. 15: Pareto-optimal networks obtained via various proxies for ImageNet16-120 dataset on NATS-Bench, and for various latency constraints on NVIDIA GTX1080. The gray points in these figures are candidate networks in the search space.

search spaces. In fact, Section 4.1 and Section 4.2 show that designing a zero-shot proxy that generally works well is extremely difficult. One potential direction for zero-shot proxies design may lie in partitioning the entire search space into several sub-spaces and then proposing customized proxies specifically designed for different sub-spaces.

5 CONCLUSION

In this paper, we have presented a comprehensive review of existing zero-shot NAS approaches. To this end, we have first introduced accuracy proxies for zero-shot NAS by providing theoretical inspirations behind these proxies and several commonly used NAS benchmarks. We then have introduced several popular approaches for hardware performance predictions. We have also compared the existing proxies against two naive proxies, namely, #Params and #FLOPs. By calculating the correlation between these proxies and the real test accuracy, we have shown that the proposed proxies to date are not necessarily better than #Params and #FLOPs for these tasks for unconstrained search spaces (*i.e.*, considering all architectures in benchmarks). However, for constrained search spaces (*i.e.*, when considering only networks with high accuracy), we revealed that the existing proxies much worse with the real accuracy including #Params and #FLOPs. Based on these analyses, we have explained why #Params work and when #Params fail. Finally, we have pointed out several potential research directions to design better NAS

benchmarks for better zero-shot NAS and multiple ideas that may enable the design of better zero-shot NAS approaches.

REFERENCES

- [1] A. Krizhevsky, I. Sutskever, and G. E. Hinton, "Imagenet classification with deep convolutional neural networks," in *Advances in Neural Information Processing Systems*, 2012.
- [2] S. Liu and W. Deng, "Very deep convolutional neural network based image classification using small training sample size," in *2015 3rd IAPR Asian Conference on Pattern Recognition (ACPR)*, 2015.
- [3] G. Huang, Z. Liu, L. Van Der Maaten, and K. Q. Weinberger, "Densely Connected Convolutional Networks," in *Proceedings of the IEEE conference on computer vision and pattern recognition*, 2017.
- [4] K. He, X. Zhang, S. Ren, and J. Sun, "Deep Residual Learning for Image Recognition," in *Proceedings of the IEEE conference on computer vision and pattern recognition*, 2016, pp. 770–778.
- [5] A. Dosovitskiy et al., "An image is worth 16x16 words: Transformers for image recognition at scale," in *International Conference on Learning Representations*, 2021.
- [6] T. B. Brown et al., "Language Models are Few-Shot Learners," *arXiv preprint arXiv:2005.14165*, 2020.
- [7] A. Vaswani, N. Shazeer, N. Parmar, J. Uszkoreit, L. Jones, A. N. Gomez, L. Kaiser, and I. Polosukhin, "Attention is all you need," *Advances in neural information processing systems*, vol. 30, 2017.
- [8] B. Baker, O. Gupta, N. Naik, and R. Raskar, "Designing Neural Network Architectures using Reinforcement Learning," *arXiv preprint arXiv:1611.02167*, 2016.
- [9] B. Zoph and Q. V. Le, "Neural Architecture Search with Reinforcement Learning," *arXiv preprint arXiv:1611.01578*, 2016.

- [10] C. Liu et al., "Progressive Neural Architecture Search," in *Proceedings of the European Conference on Computer Vision (ECCV)*, 2018.
- [11] H. Liu, K. Simonyan, and Y. Yang, "Darts: Differentiable architecture search," *arXiv preprint arXiv:1806.09055*, 2018.
- [12] T. Elsken, J. H. Metzen, and F. Hutter, "Neural architecture search: A survey," *The Journal of Machine Learning Research*, 2019.
- [13] H. Pham, M. Guan, B. Zoph, Q. Le, and J. Dean, "Efficient Neural Architecture Search via Parameters Sharing," in *International Conference on Machine Learning*. PMLR, 2018, pp. 4095–4104.
- [14] E. Real et al., "Large-scale Evolution of Image Classifiers," in *International Conference on Machine Learning*. PMLR, 2017.
- [15] X. Gong, S. Chang, Y. Jiang, and Z. Wang, "Autogan: Neural architecture search for generative adversarial networks," in *Proceedings of the IEEE/CVF International Conference on Computer Vision*, 2019, pp. 3224–3234.
- [16] S. Xie, H. Zheng, C. Liu, and L. Lin, "SNAS: stochastic neural architecture search," in *International Conference on Learning Representations*, 2019.
- [17] B. Wu et al., "Fbnet: Hardware-aware efficient convnet design via differentiable neural architecture search," in *Proceedings of the IEEE/CVF Conference on Computer Vision and Pattern Recognition*, 2019.
- [18] A. Wan, X. Dai, P. Zhang, Z. He, Y. Tian, S. Xie, B. Wu, M. Yu, T. Xu, K. Chen et al., "Fbnetv2: Differentiable neural architecture search for spatial and channel dimensions," in *Proceedings of the IEEE/CVF Conference on Computer Vision and Pattern Recognition*, 2020, pp. 12965–12974.
- [19] L. Li and A. Talwalkar, "Random search and reproducibility for neural architecture search," in *Uncertainty in artificial intelligence*. PMLR, 2020, pp. 367–377.
- [20] K. Kandasamy, W. Neiswanger, J. Schneider, B. Póczos, and E. P. Xing, "Neural architecture search with bayesian optimisation and optimal transport," *Advances in neural information processing systems*, vol. 31, 2018.
- [21] K. Yu, C. Sciuto, M. Jaggi, C. Musat, and M. Salzmann, "Evaluating the search phase of neural architecture search," *arXiv preprint arXiv:1902.08142*, 2019.
- [22] H. Liu, K. Simonyan, O. Vinyals, C. Fernando, and K. Kavukcuoglu, "Hierarchical representations for efficient architecture search," *arXiv preprint arXiv:1711.00436*, 2017.
- [23] H. Cai, T. Chen, W. Zhang, Y. Yu, and J. Wang, "Efficient architecture search by network transformation," in *Proceedings of the AAAI Conference on Artificial Intelligence*, vol. 32, no. 1, 2018.
- [24] R. Luo, F. Tian, T. Qin, E. Chen, and T.-Y. Liu, "Neural architecture optimization," *Advances in neural information processing systems*, vol. 31, 2018.
- [25] C. Zhang, M. Ren, and R. Urtasun, "Graph hypernetworks for neural architecture search," *arXiv preprint arXiv:1810.05749*, 2018.
- [26] H. Zhou, M. Yang, J. Wang, and W. Pan, "Bayesnas: A bayesian approach for neural architecture search," in *International conference on machine learning*. PMLR, 2019, pp. 7603–7613.
- [27] A. Howard, M. Sandler, G. Chu, L.-C. Chen, B. Chen, M. Tan, W. Wang, Y. Zhu, R. Pang, V. Vasudevan et al., "Searching for mobilenetv3," in *Proceedings of the IEEE/CVF international conference on computer vision*, 2019, pp. 1314–1324.
- [28] J. Yu, P. Jin, H. Liu, G. Bender, P.-J. Kindermans, M. Tan, T. Huang, X. Song, R. Pang, and Q. Le, "Bignas: Scaling up neural architecture search with big single-stage models," in *European Conference on Computer Vision*. Springer, 2020, pp. 702–717.
- [29] M. Tan, B. Chen, R. Pang, V. Vasudevan, M. Sandler, A. Howard, and Q. V. Le, "Mnasnet: Platform-aware neural architecture search for mobile," in *Proceedings of the IEEE/CVF Conference on Computer Vision and Pattern Recognition*, 2019, pp. 2820–2828.
- [30] H. Mao, M. Schwarzkopf, S. B. Venkatakrisnan, Z. Meng, and M. Alizadeh, "Learning Scheduling Algorithms for Data Processing Clusters," in *ACM Special Interest Group on Data Communication*, 2019, pp. 270–288.
- [31] W.-L. Chiang et al., "Cluster-gcn: An Efficient Algorithm for Training Deep and Large Graph Convolutional Networks," in *Proceedings of the 25th ACM SIGKDD International Conference on Knowledge Discovery & Data Mining*, 2019, pp. 257–266.
- [32] Y. Xu, L. Xie, X. Zhang, X. Chen, G.-J. Qi, Q. Tian, and H. Xiong, "Pc-darts: Partial channel connections for memory-efficient architecture search," *arXiv preprint arXiv:1907.05737*, 2019.
- [33] X. Dong and Y. Yang, "Searching for a robust neural architecture in four gpu hours," in *Proceedings of the IEEE/CVF Conference on Computer Vision and Pattern Recognition*, 2019, pp. 1761–1770.
- [34] A. Zela, T. Elsken, T. Saikia, Y. Marrakchi, T. Brox, and F. Hutter, "Understanding and robustifying differentiable architecture search," *arXiv preprint arXiv:1909.09656*, 2019.
- [35] X. Chen, L. Xie, J. Wu, and Q. Tian, "Progressive differentiable architecture search: Bridging the depth gap between search and evaluation," in *Proceedings of the IEEE/CVF international conference on computer vision*, 2019, pp. 1294–1303.
- [36] H. Cai, L. Zhu, and S. Han, "ProxylessNAS: Direct neural architecture search on target task and hardware," in *International Conference on Learning Representations*, 2019.
- [37] H. Cai, C. Gan, T. Wang, Z. Zhang, and S. Han, "Once-for-all: Train one network and specialize it for efficient deployment," in *International Conference on Learning Representations*, 2020.
- [38] Paper with code, "Neural architecture search on imagenet." <https://paperswithcode.com/sota/neural-architecture-search-on-imagenet>, 2023.
- [39] D. Stamoulis et al., "Single-Path NAS: Designing Hardware-Efficient ConvNets in less than 4 Hours," *arXiv preprint arXiv:1904.02877*, 2019.
- [40] X. Chu, B. Zhang, and R. Xu, "Fairnas: Rethinking evaluation fairness of weight sharing neural architecture search," in *Proceedings of the IEEE/CVF International Conference on Computer Vision*, 2021, pp. 12239–12248.
- [41] Z. Guo, X. Zhang, H. Mu, W. Heng, Z. Liu, Y. Wei, and J. Sun, "Single path one-shot neural architecture search with uniform sampling," in *European conference on computer vision*. Springer, 2020, pp. 544–560.
- [42] W. Chen, X. Gong, X. Liu, Q. Zhang, Y. Li, and Z. Wang, "Fasterseg: Searching for faster real-time semantic segmentation," in *International Conference on Learning Representations*, 2020.
- [43] M. Wu, H. Lin, and C. Tsai, "A training-free genetic neural architecture search," in *ACM ICEA '21: 2021 ACM International Conference on Intelligent Computing and its Emerging Applications*, Jinan, China, December 28 - 29, 2022. ACM, 2021, pp. 65–70.
- [44] Y. Shu, Z. Dai, Z. Wu, and B. K. H. Low, "Unifying and boosting gradient-based training-free neural architecture search," *CoRR*, vol. abs/2201.09785, 2022.
- [45] M. Javaheripi, S. Shah, S. Mukherjee, T. L. Religa, C. C. T. Mendes, G. H. de Rosa, S. Bubeck, F. Koushanfar, and D. Dey, "Litetransformersearch: Training-free on-device search for efficient autoregressive language models," *CoRR*, vol. abs/2203.02094, 2022.
- [46] Q. Zhou, K. Sheng, X. Zheng, K. Li, X. Sun, Y. Tian, J. Chen, and R. Ji, "Training-free transformer architecture search," *CoRR*, vol. abs/2203.12217, 2022.
- [47] T. M. Ingolfsson, M. Vero, X. Wang, L. Lamberti, L. Benini, and M. Spallanzani, "Reducing neural architecture search spaces with training-free statistics and computational graph clustering," in *CF '22: 19th ACM International Conference on Computing Frontiers*, Turin, Italy, May 17 - 22, 2022, L. Sterpone, A. Bartolini, and A. Butko, Eds. ACM, 2022, pp. 213–214.
- [48] L. T. Tran and S.-H. Bae, "Training-free hardware-aware neural architecture search with reinforcement learning," *Journal of Broadcast Engineering*, vol. 26, no. 7, pp. 855–861, 2021.
- [49] L.-T. Tran, M. S. Ali, and S.-H. Bae, "A feature fusion based indicator for training-free neural architecture search," *IEEE Access*, vol. 9, pp. 133 914–133 923, 2021.
- [50] T. Do and N. H. Luong, "Training-free multi-objective evolutionary neural architecture search via neural tangent kernel and number of linear regions," in *International Conference on Neural Information Processing*. Springer, 2021, pp. 335–347.
- [51] L. Xiang, Ł. Dudziak, M. S. Abdelfattah, T. Chau, N. D. Lane, and H. Wen, "Zero-cost proxies meet differentiable architecture search," *arXiv preprint arXiv:2106.06799*, 2021.
- [52] D. Zhou, X. Zhou, W. Zhang, C. C. Loy, S. Yi, X. Zhang, and W. Ouyang, "Econas: Finding proxies for economical neural architecture search," in *Proceedings of the IEEE/CVF Conference on computer vision and pattern recognition*, 2020, pp. 11 396–11 404.
- [53] W. Chen, X. Gong, and Z. Wang, "Neural architecture search on imagenet in four gpu hours: A theoretically inspired perspective," in *International Conference on Learning Representations*, 2021.
- [54] M. S. Abdelfattah, A. Mehrotra, Ł. Dudziak, and N. D. Lane, "Zero-cost proxies for lightweight nas," in *International Conference on Learning Representations*, 2021.

- [55] X. He, K. Zhao, and X. Chu, "Automl: A survey of the state-of-the-art," *Knowledge-Based Systems*, vol. 212, p. 106622, 2021.
- [56] M. Wistuba, A. Rawat, and T. Pedapati, "A survey on neural architecture search," *arXiv preprint arXiv:1905.01392*, 2019.
- [57] P. Ren, Y. Xiao, X. Chang, P.-Y. Huang, Z. Li, X. Chen, and X. Wang, "A comprehensive survey of neural architecture search: Challenges and solutions," *ACM Computing Surveys (CSUR)*, 2021.
- [58] Y. Liu, Y. Sun, B. Xue, M. Zhang, G. G. Yen, and K. C. Tan, "A survey on evolutionary neural architecture search," *IEEE transactions on neural networks and learning systems*, 2021.
- [59] L. Xie, X. Chen, K. Bi, L. Wei, Y. Xu, L. Wang, Z. Chen, A. Xiao, J. Chang, X. Zhang, and Q. Tian, "Weight-sharing neural architecture search: A battle to shrink the optimization gap," *ACM Comput. Surv.*, vol. 54, no. 9, oct 2021.
- [60] H. Benmeziane, K. El Maghraoui, H. Ouarnoughi, S. Niar, M. Wistuba, and N. Wang, "Hardware-aware neural architecture search: Survey and taxonomy," in *Proceedings of the Thirtieth International Joint Conference on Artificial Intelligence, IJCAI-21*, Z.-H. Zhou, Ed. International Joint Conferences on Artificial Intelligence Organization, 8 2021, pp. 4322–4329, survey Track.
- [61] C. White, M. Khodak, R. Tu, S. Shah, S. Bubeck, and D. Dey, "A deeper look at zero-cost proxies for lightweight nas," in *ICLR Blog Track, 2022*, <https://iclr-blog-track.github.io/2022/03/25/zero-cost-proxies/>. [Online]. Available: <https://iclr-blog-track.github.io/2022/03/25/zero-cost-proxies/>
- [62] X. Ning, C. Tang, W. Li, Z. Zhou, S. Liang, H. Yang, and Y. Wang, "Evaluating efficient performance estimators of neural architectures," in *Advances in Neural Information Processing Systems 34: Annual Conference on Neural Information Processing Systems 2021, NeurIPS 2021, December 6-14, 2021, virtual*, M. Ranzato, A. Beygelzimer, Y. N. Dauphin, P. Liang, and J. W. Vaughan, Eds., 2021, pp. 12 265–12 277.
- [63] N. Lee, T. Ajanthan, and P. Torr, "SNIP: SINGLE-SHOT NETWORK PRUNING BASED ON CONNECTION SENSITIVITY," in *International Conference on Learning Representations*, 2019.
- [64] H. Tanaka, D. Kunin, D. L. Yamins, and S. Ganguli, "Pruning neural networks without any data by iteratively conserving synaptic flow," in *Advances in Neural Information Processing Systems*, H. Larochelle, M. Ranzato, R. Hadsell, M. Balcan, and H. Lin, Eds., vol. 33. Curran Associates, Inc., 2020, pp. 6377–6389.
- [65] C. Wang, G. Zhang, and R. B. Grosse, "Picking winning tickets before training by preserving gradient flow," in *8th International Conference on Learning Representations, ICLR 2020, Addis Ababa, Ethiopia, April 26-30, 2020*. OpenReview.net, 2020.
- [66] P. Molchanov, A. Mallya, S. Tyree, I. Frosio, and J. Kautz, "Importance estimation for neural network pruning," in *IEEE Conference on Computer Vision and Pattern Recognition, CVPR 2019, Long Beach, CA, USA, June 16-20, 2019*. Computer Vision Foundation / IEEE, 2019, pp. 11 264–11 272.
- [67] L. Liu, S. Zhang, Z. Kuang, A. Zhou, J. Xue, X. Wang, Y. Chen, W. Yang, Q. Liao, and W. Zhang, "Group fisher pruning for practical network compression," in *Proceedings of the 38th International Conference on Machine Learning, ICML 2021, 18-24 July 2021, Virtual Event, ser. Proceedings of Machine Learning Research*, M. Meila and T. Zhang, Eds., vol. 139. PMLR, 2021, pp. 7021–7032.
- [68] V. Lopes, S. Alirezazadeh, and L. A. Alexandre, "Epe-nas: Efficient performance estimation without training for neural architecture search," in *International Conference on Artificial Neural Networks*. Springer, 2021, pp. 552–563.
- [69] J. Mellor, J. Turner, A. Storkey, and E. J. Crowley, "Neural architecture search without training," in *International Conference on Machine Learning*. PMLR, 2021, pp. 7588–7598.
- [70] M. Lin, P. Wang, Z. Sun, H. Chen, X. Sun, Q. Qian, H. Li, and R. Jin, "Zen-nas: A zero-shot nas for high-performance image recognition," in *Proceedings of the IEEE/CVF International Conference on Computer Vision*, 2021, pp. 347–356.
- [71] Z. Sun, M. Lin, Z. Tan, X. Sun, and R. Jin, "Zenet: Revisiting efficient object detection backbones from zero-shot neural architecture search," 2021.
- [72] L. Chizat, E. Oyallon, and F. R. Bach, "On lazy training in differentiable programming," in *Advances in Neural Information Processing Systems 32: Annual Conference on Neural Information Processing Systems 2019, NeurIPS 2019, December 8-14, 2019, Vancouver, BC, Canada*, H. M. Wallach, H. Larochelle, A. Beygelzimer, F. d'Alché-Buc, É. B. Fox, and R. Garnett, Eds., 2019, pp. 2933–2943.
- [73] A. Jacot, C. Hongler, and F. Gabriel, "Neural tangent kernel: Convergence and generalization in neural networks," in *Advances in Neural Information Processing Systems 31: Annual Conference on Neural Information Processing Systems 2018, NeurIPS 2018, December 3-8, 2018, Montréal, Canada*, S. Bengio, H. M. Wallach, H. Larochelle, K. Grauman, N. Cesa-Bianchi, and R. Garnett, Eds., 2018.
- [74] J. Lee, L. Xiao, S. S. Schoenholz, Y. Bahri, R. Novak, J. Sohl-Dickstein, and J. Pennington, "Wide neural networks of any depth evolve as linear models under gradient descent," in *Advances in Neural Information Processing Systems 32: Annual Conference on Neural Information Processing Systems 2019, NeurIPS 2019, December 8-14, 2019, Vancouver, BC, Canada*, H. M. Wallach, H. Larochelle, A. Beygelzimer, F. d'Alché-Buc, É. B. Fox, and R. Garnett, Eds., 2019, pp. 8570–8581.
- [75] W. Chen, W. Huang, X. Du, X. Song, Z. Wang, and D. Zhou, "Auto-scaling vision transformers without training," in *International Conference on Learning Representations*, 2022.
- [76] M. Raghu, B. Poole, J. M. Kleinberg, S. Ganguli, and J. Sohl-Dickstein, "On the expressive power of deep neural networks," in *Proceedings of the 34th International Conference on Machine Learning, ICML 2017, Sydney, NSW, Australia, 6-11 August 2017, ser. Proceedings of Machine Learning Research*, D. Precup and Y. W. Teh, Eds., vol. 70. PMLR, 2017, pp. 2847–2854.
- [77] T. Serra, C. Tjandraatmadja, and S. Ramalingam, "Bounding and counting linear regions of deep neural networks," in *Proceedings of the 35th International Conference on Machine Learning, ICML 2018, Stockholm, Sweden, July 10-15, 2018, ser. Proceedings of Machine Learning Research*, J. G. Dy and A. Krause, Eds., vol. 80. PMLR, 2018, pp. 4565–4573.
- [78] B. Hanin and D. Rolnick, "Complexity of linear regions in deep networks," in *Proceedings of the 36th International Conference on Machine Learning, ICML 2019, 9-15 June 2019, Long Beach, California, USA, ser. Proceedings of Machine Learning Research*, K. Chaudhuri and R. Salakhutdinov, Eds. PMLR, 2019.
- [79] H. Xiong, L. Huang, M. Yu, L. Liu, F. Zhu, and L. Shao, "On the number of linear regions of convolutional neural networks," in *Proceedings of the 37th International Conference on Machine Learning, ICML 2020, 13-18 July 2020, Virtual Event, ser. Proceedings of Machine Learning Research*. PMLR, 2020.
- [80] K. Bhardwaj, G. Li, and R. Marculescu, "How does topology influence gradient propagation and model performance of deep networks with densenet-type skip connections?" in *IEEE Conference on Computer Vision and Pattern Recognition, CVPR 2021, virtual, June 19-25, 2021*. Computer Vision Foundation / IEEE, 2021.
- [81] K. Bhardwaj, J. Ward, C. Tung, D. Gope, L. Meng, I. Fedorov, A. Chalfin, P. Whatmough, and D. Loh, "Restructurable activation networks," *arXiv preprint arXiv:2208.08562*, 2022.
- [82] G. Li, S. K. Mandal, Ü. Y. Ogras, and R. Marculescu, "FLASH: fast neural architecture search with hardware optimization," *ACM Trans. Embed. Comput. Syst.*, vol. 20, no. 5s, pp. 63:1–63:26, 2021.
- [83] W. Chen, W. Huang, X. Gong, B. Hanin, and Z. Wang, "Deep architecture connectivity matters for its convergence: A fine-grained analysis," in *Advances in Neural Information Processing Systems*, A. H. Oh, A. Agarwal, D. Belgrave, and K. Cho, Eds., 2022.
- [84] J. Lee, J. Sohl-dickstein, J. Pennington, R. Novak, S. Schoenholz, and Y. Bahri, "Deep neural networks as gaussian processes," in *International Conference on Learning Representations*, 2018.
- [85] J. Siems, L. Zimmer, A. Zela, J. Lukasik, M. Keuper, and F. Hutter, "Nas-bench-301 and the case for surrogate benchmarks for neural architecture search," *arXiv preprint arXiv:2008.09777*, 2020.
- [86] Y. Mehta, C. White, A. Zela, A. Krishnakumar, G. Zaberger, S. Moradian, M. Safari, K. Yu, and F. Hutter, "Nas-bench-suite: Nas evaluation is (now) surprisingly easy," *arXiv preprint arXiv:2201.13396*, 2022.
- [87] A. Mehrotra, A. G. C. Ramos, S. Bhattacharya, Ł. Dudziak, R. Vipperla, T. Chau, M. S. Abdelfattah, S. Ishtiaq, and N. D. Lane, "Nas-bench-asr: Reproducible neural architecture search for speech recognition," in *International Conference on Learning Representations*, 2020.
- [88] N. Klyuchnikov, I. Trofimov, E. Artemova, M. Salnikov, M. Fedorov, A. Filippov, and E. Burnaev, "Nas-bench-nlp: neural architecture search benchmark for natural language processing," *IEEE Access*, vol. 10, pp. 45 736–45 747, 2022.
- [89] C. Ying, A. Klein, E. Christiansen, E. Real, K. Murphy, and F. Hutter, "Nas-bench-101: Towards reproducible neural architecture search,"

- in International Conference on Machine Learning. PMLR, 2019, pp. 7105–7114.
- [90] X. Dong and Y. Yang, “NAS-Bench-201: Extending the Scope of Reproducible Neural Architecture Search,” arXiv preprint arXiv:2001.00326, 2020.
- [91] X. Dong, L. Liu, K. Musial, and B. Gabrys, “Nats-bench: Benchmarking nas algorithms for architecture topology and size,” IEEE transactions on pattern analysis and machine intelligence, 2021.
- [92] Y. Duan, X. Chen, H. Xu, Z. Chen, X. Liang, T. Zhang, and Z. Li, “Transnas-bench-101: Improving transferability and generalizability of cross-task neural architecture search,” in IEEE Conference on Computer Vision and Pattern Recognition, CVPR 2021, virtual, June 19-25, 2021. Computer Vision Foundation / IEEE, 2021.
- [93] C. Li, Z. Yu, Y. Fu, Y. Zhang, Y. Zhao, H. You, Q. Yu, Y. Wang, and Y. Lin, “Hw-nas-bench: Hardware-aware neural architecture search benchmark,” arXiv preprint arXiv:2103.10584, 2021.
- [94] L. Dudziak, T. Chau, M. S. Abdelfattah, R. Lee, H. Kim, and N. D. Lane, “BRP-NAS: prediction-based NAS using gcns,” in Advances in Neural Information Processing Systems 33: Annual Conference on Neural Information Processing Systems 2020, NeurIPS 2020, December 6-12, 2020, virtual, H. Larochelle, M. Ranzato, R. Hadsell, M. Balcan, and H. Lin, Eds., 2020.
- [95] H. Lee, S. Lee, S. Chong, and S. J. Hwang, “Hardware-adaptive efficient latency prediction for nas via meta-learning,” in Advances in Neural Information Processing Systems, M. Ranzato, A. Beygelzimer, Y. Dauphin, P. Liang, and J. W. Vaughan, Eds., 2021.
- [96] L. L. Zhang, S. Han, J. Wei, N. Zheng, T. Cao, Y. Yang, and Y. Liu, “nn-meter: towards accurate latency prediction of deep-learning model inference on diverse edge devices,” in MobiSys '21: The 19th Annual International Conference on Mobile Systems, Applications, and Services, Virtual Event, Wisconsin, USA, 24 June - 2 July, 2021, S. Banerjee, L. Mottola, and X. Zhou, Eds. ACM, 2021, pp. 81–93.
- [97] K. Bhardwaj, G. Li, and R. Marculescu, “How does topology influence gradient propagation and model performance of deep networks with densenet-type skip connections?” in Proceedings of the IEEE/CVF Conference on Computer Vision and Pattern Recognition (CVPR), 2021.
- [98] N. Tripuraneni, B. Adlam, and J. Pennington, “Overparameterization improves robustness to covariate shift in high dimensions,” Advances in Neural Information Processing Systems, 2021.
- [99] P. Langley, “Crafting papers on machine learning,” in Proceedings of the 17th International Conference on Machine Learning (ICML 2000), P. Langley, Ed. Stanford, CA: Morgan Kaufmann, 2000.